



## Measurements of $W$ and $Z$ boson production in association with jets in proton-proton collisions with the ATLAS detector

Gavin Hesketh, on behalf of the ATLAS Collaboration

*University College London, Gower Street, London, WC1E 6BT, UK*

*[gavin.hesketh@ucl.ac.uk](mailto:gavin.hesketh@ucl.ac.uk)*

---

### Abstract

The latest measurements of the production of  $W$  or  $Z$  boson in association with jets by the ATLAS detector are reported. A data-set of proton-proton collisions corresponding to an integrated luminosity of approximately  $4.6 \text{ fb}^{-1}$  have been analysed, and new results of  $W$  boson + jet production, the ratio of  $W$  to  $Z$  boson + jet production,  $W$  boson + charm, and  $Z$  boson +  $b$ -jet production are described. Extensive comparisons from the latest theoretical calculations are also included.

*Keywords:* QCD, ATLAS, V+jets, LHC, CERN

---

### 1. Introduction

The electron and muon decay modes of the  $W$  and  $Z$  boson give clear experimental signatures in the high occupancy environment of hadron collisions. They therefore make ideal tools with which to probe the underlying hadronic interaction. The production of jets in addition to the  $W$  or  $Z$  boson can lead to complex, multi-object final states which are not only difficult to calculate in QCD, but also act as a dominant background in many other analyses. Studying such events therefore tests our understanding of fundamental physics, but also increases our sensitivity to studies and searches for rare or new phenomena.

To obtain the best description of multi-jet final states, explicit matrix element calculations are required, evolved to particle level by interfacing to parton shower event generators. In order to obtain a complete sample, these matrix element calculations with different jet multiplicities must be merged; this merging can introduce overlaps between configurations generated by different ME+PS samples. Methods for dealing with these overlaps, such as MLM [1] and CKKW [2] have been available for some time. Moving to next-to-leading or-

der matrix element calculations, additional complications appear in the matching and merging of samples, and a range of new techniques are under development to deal with this. Comparisons to precise measurements will determine which techniques gives the most accurate description of data, or highlight where more tuning is needed.

For the production of heavy flavour, studying  $W$ +charm production brings sensitivity to another area: PDFs, particularly the strange content of the proton. In  $b$  production, the mass of the  $b$ -quark adds further complications. Production of  $b$  can be handled in PDFs (5 flavour scheme) or in the matrix element (4 flavour scheme), with a different treatment of the  $b$  mass in each case. Calculations in the 4 flavour scheme are also more complex to match and merge, while still covering the full kinematic phase space.

This note summarises recent measurements of V+jet production by the ATLAS experiment [3] at the Large Hadron Collider (LHC). The measurements are made using a sample of proton-proton collisions at a centre of mass energy of  $\sqrt{s} = 7 \text{ TeV}$ , corresponding to a luminosity of just under  $5 \text{ fb}^{-1}$ . The new results include differential cross sections in  $W$ +jet production, the ratio



of  $W$  to  $Z$ +jet production,  $W$ +charm, and  $Z + b(b)$ .

## 2. $W$ +jets

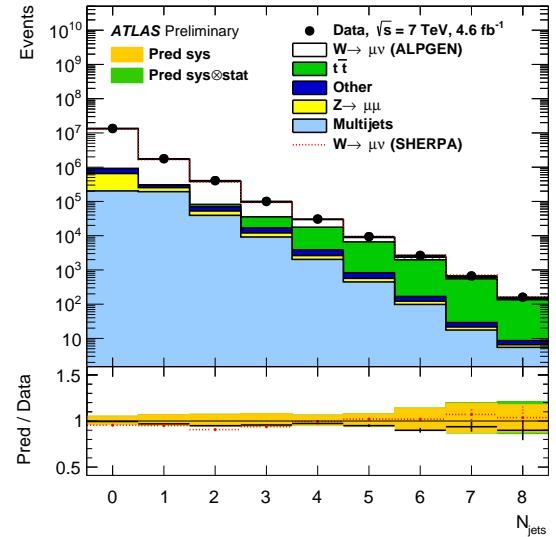
A new measurement of  $W$ +jet production was presented [4]. A sample of  $W$ +jet events are selected by requiring an electron or muon with  $p_T > 25$  GeV, and  $|\eta| < 2.5$ . To reconstruct the neutrino, missing transverse energy above 30 GeV is required. Jets are reconstructed using the anti-kt algorithm [5], with a distance parameter  $R = 0.4$ . The dominant backgrounds come from multijet production giving rise to a fake lepton signature in the detector, and, at higher jet multiplicities, top pair production. These backgrounds are estimated using data-driven techniques, and smaller backgrounds (single-top,  $Z$  boson, and diboson production) are estimated using simulation. The variation of backgrounds with jet multiplicity can be seen in Fig. 1. The background subtracted data are corrected to the particle level using a Bayesian unfolding technique [6], and particle level fiducial cross sections are presented.

The large sample is used to study numerous kinematic variables, including multiplicities up to 7 jets, and jet transverse momenta up to 1 TeV. The  $W$  cross section is measured differential in jet  $p_T$  and rapidity for the leading, second, third and fourth jet;  $\Delta\phi(\text{jet},\text{jet})$ ,  $\Delta\eta(\text{jet},\text{jet})$  and  $\Delta R(\text{jet},\text{jet})$ , the invariant mass for the leading and second jets, and  $H_T$ , the scalar sum of transverse energies of all particles in the fiducial region in the event. Figure 1 shows the leading jet  $p_T$ , while Figure 2 shows the  $H_T$  and  $\Delta\phi(\text{jet},\text{jet})$  distributions. Comparisons are made using a merged sample of NLO matrix elements produced with BLACKHAT+SHERPA [7, 8, 9]; an approximate NNLO sample produced with LoopSim [10]; merged samples using LO matrix elements produced with ALPGEN [11] and SHERPA [12]; and MEPS@NLO [13] a merged sample using NLO matrix elements calculated in SHERPA. In observables with at least two jets, comparisons are also made using HEJ [14, 15], an approximate all-orders calculation which becomes exact for very well separated jets. BLACKHAT, HEJ and MEPS@NLO are shown with uncertainty based on the choice of scale, and PDF.

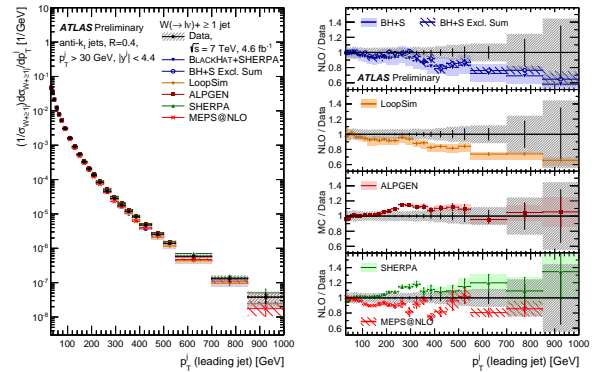
In general, a good description of the data is obtained from all theoretical predictions, though with some room for further fine tuning in each.

## 3. $R$ +jets

A more precise measurement can be obtained by taking the ratio  $R = \sigma(W + \text{jets})/\sigma(Z + \text{jets})$ . Due to the



(a)



(b)

Figure 1: 1(a): composition at detector level of the sample of events passing the  $W$ +jet selection criteria, as a function of jet multiplicity [4]. 1(b): cross section differential in the leading jet transverse momentum [4].

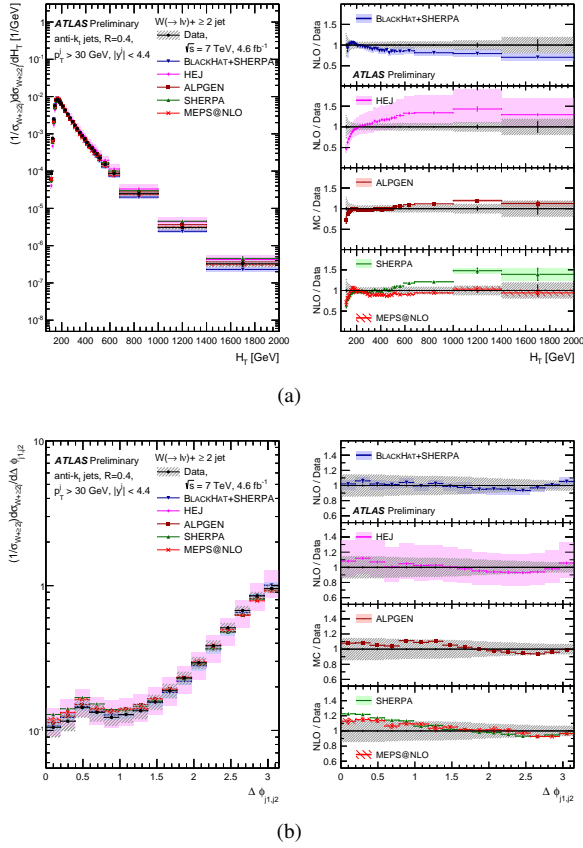


Figure 2:  $W$ +jet cross section measurements [4], differential in  $H_T$  (2(a)) and differential in  $\Delta\phi(\text{jet},\text{jet})$  (2(b)).

similarity in detector signatures, there is significant cancellation of experimental systematic uncertainties when taking this ratio. There is also a cancellation of uncertainties in calculations of  $R$ , due to the similarity of contributing processes in  $W$  and  $Z$  production. The ratio itself is sensitive to differences in jet production in  $W$  and  $Z$  events, which are driven by the mass difference between the bosons, and different quark-gluon and quark-antiquark initial states involved in  $W$  and  $Z$  boson production. At high energies, the mass difference becomes less significant, and the ratio is sensitive to any new physics contributions preferentially producing  $W$  or  $Z$  boson signatures.

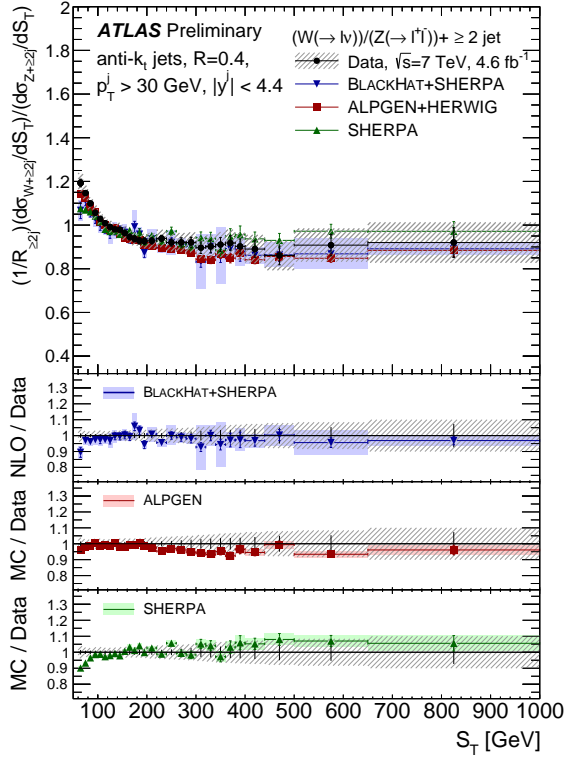
In the latest measurement from ATLAS [16], the ratio  $R$  is measured as a function of the number of jets (up to  $\geq 4$ ), the  $n^{\text{th}}$  jet  $p_T$  and rapidity,  $S_T$  (the scalar sum of jet transverse momenta),  $\Delta R(\text{jet}, \text{jet})$  and  $\Delta\phi(\text{jet}, \text{jet})$  and dijet invariant mass. Figure 3 shows  $R$  as a function of  $S_T$ , and leading jet rapidity. Comparisons are made using BLACKHAT+SHERPA, ALPGEN+HERWIG, and SHERPA. In general the description of the data is good, though there is evidence for a slope in jet rapidity in the ratio of ALPGEN to data.

#### 4. $W$ +charm

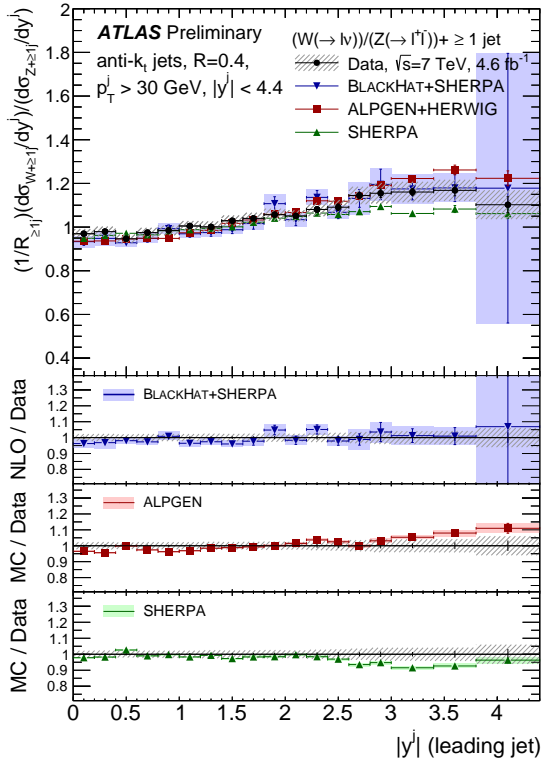
The production of a  $W$  boson and single jet containing charm is dominated by the leading order process of  $W$  boson radiation from a strange quark. Measurements of  $W$ +charm at the LHC are therefore sensitive to the strange PDF at momentum fractions  $x \approx 0.01$ , and allow tests of the impact of the strange mass on the SU(3) flavour symmetry of QCD.

A new measurement of  $W$ +charm production from ATLAS [17] uses 6 channels:  $W^\pm + c\text{-jet}$ ,  $W^\pm + D$ ,  $W^\pm + D^*$ . For the  $W + c$  channel, jets containing charm are “tagged” by reconstructing a muon from the semi-leptonic decay of a charmed hadron. The other channels reconstruct  $D$  hadrons, or pions from the decay  $D^* \rightarrow D\pi$ , based on track information. All channels rely on the charge anti-correlation between the lepton from the  $W$  boson decay and the muon in the charm jet or the  $D$  hadron. As most backgrounds are symmetric in charge configurations, the same-sign (SS) events are subtracted from the opposite-sign (OS), giving a sample greatly enhanced in signal. From this sample, inclusive and differential cross sections are extracted.

Figure 4 shows the inclusive  $W + c\text{-jet}$  OS-SS cross section, with comparisons from a NLO prediction obtained using aMC@NLO [18] interfaced to the CT10 [19], MSTW2008 [20], HERAPDF1.5 [21], ATLAS-epWZ12 [22], and NNPDF2.3coll [23] PDF



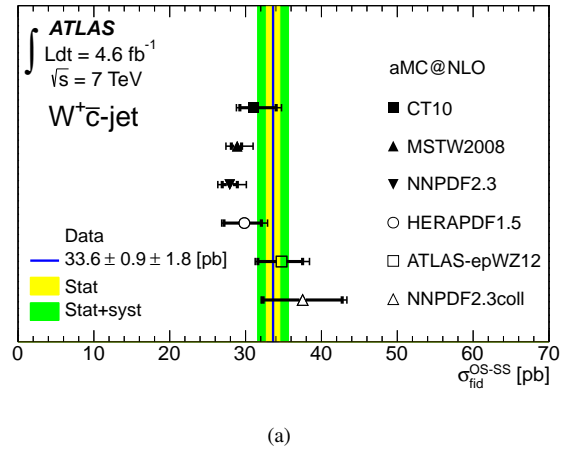
(a)



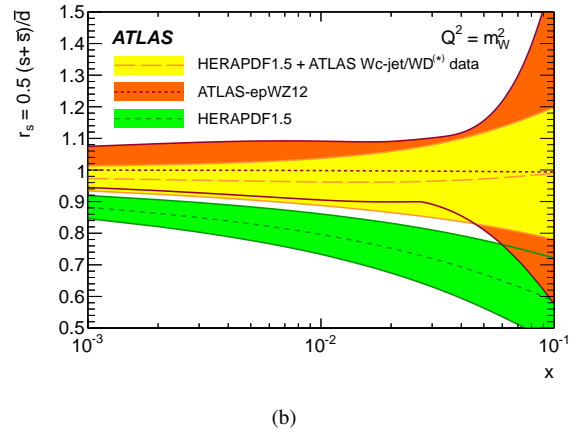
(b)

Figure 3: The ratio  $R$  [16] as a function of  $S_T$  (3(a)) and leading jet rapidity (3(b))

sets. The best description of the data is obtained using PDF sets which assume the strange sea distribution is symmetric. Also shown is the ratio of strange to down sea-quark distributions,  $r_s = 0.5(s+\bar{s})/\bar{d}$ , as found in the HERAPDF1.5 PDF set, the ATLAS-epWZ12 PDF set, and as obtained in an updated HERAPDF fit using the  $W$ +charm data. It can be seen that the new results prefer a value of  $r_s$  up towards unity, implying a symmetric sea.



(a)



(b)

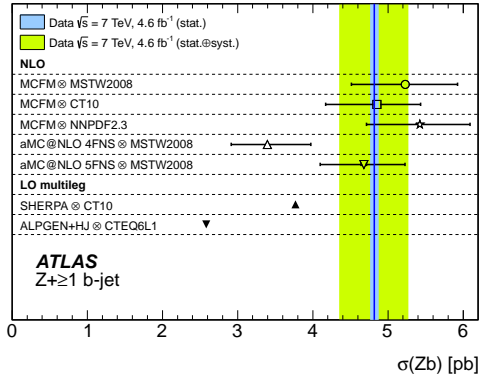
Figure 4: 4(a): The  $W+c$ -jet cross section compared to theoretical predictions using different PDFs [17]. 4(b): Ratio of the strange to down sea-quark distributions in HERAPDF1.5 PDF, compared to the ratio obtained from the fit including the ATLAS  $W+c$ -jet/ $WD^{(*)}$  data and the ratio obtained from the ATLAS-epWZ12 PDF set [17].

## 5. $Z + b(b)$

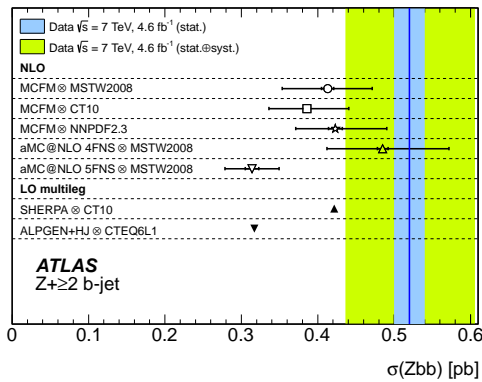
A new measurement of  $Z+b$ -jets was also presented, including inclusive and differential cross sections for  $Z + \geq 1b$ -jet and  $Z + \geq 2b$ -jets [24]. The modelling

of these final states can be achieved using different approaches, with either a  $b$  PDF in the proton (5-flavour scheme) or not (4-flavour scheme), which also differ in the treatment of the  $b$  mass, and require different matching criteria in combined ME+PS samples. The kinematics of the  $b$ -jet and  $Z$  boson provide a test of these theoretical predictions.

Figure 5 shows the inclusive cross sections, with comparisons from MCFM [25, 26], a parton level prediction with non-perturbative corrections derived using SHERPA; 4-flavour and 5-flavour predictions from aMC@NLO [27]; and ALPGEN and SHERPA LO multi-leg predictions. The best description of the data is obtained from MCFM, while the 4-flavour and 5-flavour aMC@NLO predictions show different levels of agreement in the  $Z+ \geq 1b$ -jet and  $Z+ \geq 2b$ -jet cases.



(a)



(b)

Figure 5: The inclusive fiducial cross section for 5(a)  $Z+ \geq 1b$ -jet [24] and 5(b)  $Z+ \geq 2b$ -jets [24].

A number of differential cross sections testing a range of kinematic variables are also measured, including the  $b$ -jet  $p_T$  and rapidity, the  $\Delta R$ ,  $\Delta\phi$ ,  $\Delta y$  and  $y_{boost}$  of the  $Z$

and any  $b$ -jets, the  $Z$   $p_T$  and rapidity in events containing  $\geq 1$  and  $\geq 2$   $b$ -jets, and the invariant mass of the two leading  $b$ -jets in any event. To test for possible sensitivity to the  $b$  PDF, the cross section for  $Z+ \geq 1b$ -jet production, differential in  $Z$  rapidity, is shown in Figure 6. Predictions using different PDF sets are compared to the data, and while the uncertainty on the theoretical predictions is dominated by the scale uncertainty, a clear trend is visible in the ratio indicating these data may be used in future PDF fits.

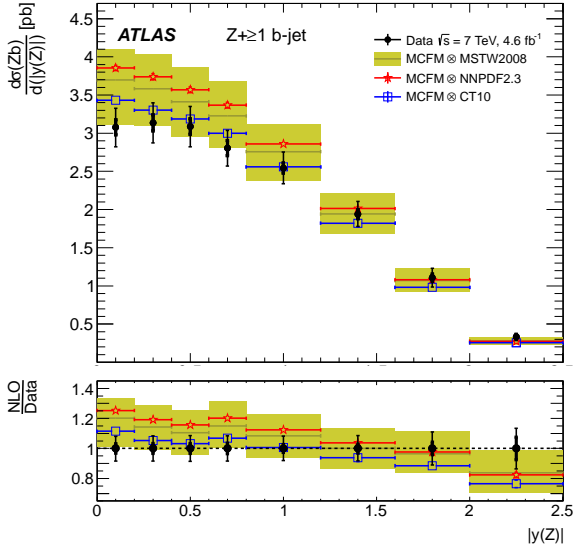
Figure 6 also shows the cross section for  $Z+ \geq 2b$ -jet events, differential in  $\Delta R(b\text{-jet}, b\text{-jet})$ . The shape of the data is generally described well by the theoretical predictions, though there is some indication of a disagreement at low  $\Delta R$ , a region dominated by  $g \rightarrow bb$ , a process of particular interest as a source of background events to Higgs decays to  $b$ -quarks.

## 6. Conclusions

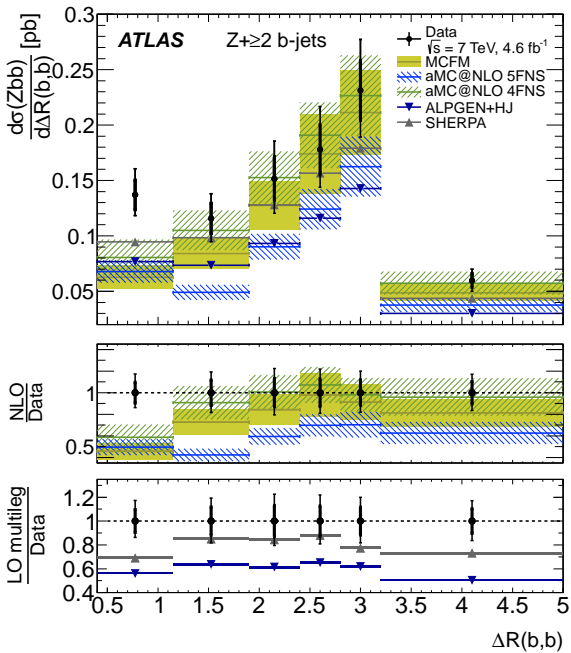
The production of  $W$  or  $Z$  bosons in association with jets are basic physics signals at the LHC, and make an excellent test signal for our understanding of fundamental physics, and our ability to model complex final states. These signals also frequently form the background to other analyses for new or rare signals like the Higgs boson, where improving the modelling is crucial. The latest results from ATLAS continue to push forward with new levels of precision, reaching into new kinematic regimes, and exploring new variables. While the general description by theory are good, there are areas for further tuning in all of the analyses shown.

## References

- [1] J. Alwall, et al., Comparative study of various algorithms for the merging of parton showers and matrix elements in hadronic collisions, Eur. Phys. J. C53 (2008) 473. arXiv:0706.2569.
- [2] S. Catani, F. Krauss, R. Kuhn, B. R. Webber, QCD Matrix elements + parton showers, JHEP 11 (2011) 063. arXiv:hep-ph/0109231.
- [3] ATLAS collaboration, The ATLAS Experiment at the CERN Large Hadron Collider, JINST 3 (2008) S08003. URL <https://cds.cern.ch/record/1129811>
- [4] ATLAS collaboration, Measurements of the  $W$  production cross sections in association with jets with the ATLAS detector, Submitted to EPJ C. arXiv:1409.8639.
- [5] M. Cacciari, G. P. Salam, G. Soyez, The anti- $k_r$  jet clustering algorithm, JHEP 0804 (2008) 063. arXiv:0802.1189.
- [6] G. D'Agostini, A Multidimensional unfolding method based on Bayes' theorem, Nucl. Instrum. Meth. A362 (1995) 487–498.
- [7] C. Berger, Z. Bern, L. J. Dixon, F. Febres Cordero, D. Forde, et al., Next-to-Leading Order QCD Predictions for  $W+3$ -Jet Distributions at Hadron Colliders, Phys.Rev. D80 (2009) 074036. arXiv:0907.1984, doi:10.1103/PhysRevD.80.074036.



(a)



(b)

Figure 6: The fiducial cross section for 5(a)  $Z + \geq 1b$ -jet, differential in  $Z$  boson rapidity [24], and 6(b)  $Z + \geq 2b$ -jets, differential in  $\Delta R(b, b$ -jet) [24].

- [8] C. Berger, Z. Bern, L. J. Dixon, F. Febres Cordero, D. Forde, et al., Precise Predictions for  $W + 4$  Jet Production at the Large Hadron Collider, *Phys.Rev.Lett.* 106 (2011) 092001. arXiv:1009.2338, doi:10.1103/PhysRevLett.106.092001.
- [9] Z. Bern, L. Dixon, F. Febres Cordero, S. Hche, H. Ita, et al., Next-to-Leading Order  $W + 5$ -Jet Production at the LHC, *Phys.Rev.* D88 (1) (2013) 014025. arXiv:1304.1253, doi:10.1103/PhysRevD.88.014025.
- [10] M. Rubin, G. P. Salam, S. Sapeta, Giant QCD K-factors beyond NLO, *JHEP* 1009 (2010) 084. arXiv:1006.2144, doi:10.1007/JHEP09(2010)084.
- [11] M. L. Mangano, et al., ALPGEN, a generator for hard multiparton processes in hadronic collisions, *JHEP* 0307 (2003) 001. arXiv:hep-ph/0206293.
- [12] T. Gleisberg, et al., Event generation with SHERPA 1.1, *JHEP* 0902 (2009) 007. arXiv:0811.4622.
- [13] S. Hoeche, F. Krauss, M. Schonherr, F. Siegert, QCD matrix elements + parton showers: The NLO case, *JHEP* 1304 (2013) 027. arXiv:1207.5030, doi:10.1007/JHEP04(2013)027.
- [14] J. R. Andersen, J. M. Smillie, Constructing All-Order Corrections to Multi-Jet Rates, *JHEP* 1001 (2010) 039. arXiv:0908.2786, doi:10.1007/JHEP01(2010)039.
- [15] J. R. Andersen, T. Hapola, J. M. Smillie,  $W$  Plus Multiple Jets at the LHC with High Energy Jets, *JHEP* 1209 (2012) 047. arXiv:1206.6763, doi:10.1007/JHEP09(2012)047.
- [16] ATLAS collaboration, A measurement of the ratio of the production cross sections for  $W$  and  $Z$  bosons in association with jets with the ATLAS detector, Submitted to EPJ C. arXiv:1408.6510.
- [17] ATLAS collaboration, Measurement of the production of a  $W$  boson in association with a charm quark in  $pp$  collisions at  $\sqrt{s} = 7$  TeV with the ATLAS detector, *JHEP* 1405 (2014) 068. arXiv:1402.6263, doi:10.1007/JHEP05(2014)068.
- [18] J. Alwall, et al., The automated computation of tree-level and next-to-leading order differential cross sections, and their matching to parton shower simulations, *JHEP* 07 (2014) 079. arXiv:1405.0301.
- [19] H. L. Lai, et al., New parton distributions for collider physics, *Phys. Rev. D* 82 (2010) 074024. arXiv:1007.2241.
- [20] A. Martin, W. Stirling, R. Thorne, G. Watt, Parton distributions for the LHC, *Eur. Phys. J.* C63 (2009) 189–285. arXiv:0901.0002.
- [21] F. Aaron, et al., Combined Measurement and QCD Analysis of the Inclusive  $e^+p$  Scattering Cross Sections at HERA, *JHEP* 1001 (2010) 109. arXiv:0911.0884, doi:10.1007/JHEP01(2010)109.
- [22] ATLAS collaboration, Determination of the strange quark density of the proton from ATLAS measurements of the  $W \rightarrow \ell\nu$  and  $Z \rightarrow \ell\ell$  cross sections, *Phys.Rev.Lett.* 109 (2012) 012001. arXiv:1203.4051, doi:10.1103/PhysRevLett.109.012001.
- [23] R. D. Ball, et al., Parton distributions with LHC data, *Nucl. Phys.* B867 (2013) 244–289. arXiv:1207.1303.
- [24] ATLAS collaboration, Measurement of differential production cross-sections for a  $Z$  boson in association with  $b$ -jets in 7 TeV proton-proton collisions with the ATLAS detector, Submitted to JHEP. arXiv:1407.3643.
- [25] J. M. Campbell, R. Ellis, F. Maltoni, S. Willenbrock, Associated production of a  $Z$  Boson and a single heavy quark jet, *Phys. Rev. D* 69 (2004) 074021. arXiv:hep-ph/0312024.
- [26] J. M. Campbell, R. Ellis, F. Maltoni, S. Willenbrock, Production of a  $Z$  boson and two jets with one heavy quark tag, *Phys. Rev. D* 73 (2006) 054007. arXiv:hep-ph/0510362.
- [27] R. Frederix, S. Frixione, V. Hirschi, F. Maltoni, R. Pittau, P. Torrielli,  $W$  and  $Z/\gamma^*$  boson production in association with a bottom-antibottom pair, *JHEP* 09 (2011) 061. arXiv:1106.6019.